Muon spin rotation study of the layered oxyselenide $Sr_2CoO_2Ag_2Se_2$

G. J. W. Gill,[1,2,*] J. M. Wilkinson,[1] F. Lang,[1,2] J. N. Blandy,[3] S. J. Clarke,[3] and S. J. Blundell[1,†]

[1]*Clarendon Laboratory, University of Oxford Department of Physics, Parks Road, Oxford OX1 3PU, United Kingdom*

[2]*ISIS Facility, Rutherford Appleton Laboratory, Chilton, Oxfordshire OX11 0QX, United Kingdom*

[3]*Department of Chemistry, University of Oxford, Inorganic Chemistry Laboratory, South Parks Road, Oxford OX1 3QR, United Kingdom*

(Received 24 February 2022; revised 26 July 2022; accepted 28 November 2022; published 12 December 2022)

The results of a muon spin rotation experiment on the layered oxyselenide $Sr_2CoO_2Ag_2Se_2$ are presented. The compound contains square-planar CoO_2 layers and is found to exhibit a phase transition at 160.4(1) K to an antiferromagnetic configuration of the Co^{2+} ions. Density functional theory calculations were performed in order to determine the stopping site of the muon within the unit cell. The calculated magnetic dipole field at the muon stopping site was shown to be consistent with the proposed magnetic structure.

DOI: 10.1103/PhysRevB.106.224410

I. INTRODUCTION

The layered cobalt oxychalcogenides $A_2CoO_2M_2Ch_2$ (A = Sr, Ba; M = Cu, Ag; Ch = Se, S, Te) have received significant interest due to their unusual magnetic and electronic properties [1–7]. In this family of compounds, the more polarizable chalcogenide anion bonds to the metal atom, forming $(M_2Ch_2)^{2-}$ antifluorite-type layers; the less polarizable oxide anion bonds to the Co^{2+} cation to form square planar $(CoO_2)^{2-}$ layers. The resulting sandwich structures formed by alternating these layers (and known as the $Sr_2Mn_3Sb_2O_2$ structure [8]) give rise to many types of magnetic behavior as the various ions are varied. For example, the layered cobalt oxysulfides exhibit successive magnetic phase transitions and spin-glass behavior at low temperatures, and were the first compounds to realize a structure based on square planar CoO_2 layers [1].

In this paper we focus on an example of this family in which M=Ag, Ch=Se, and A=Sr. Thus, $Sr_2CoO_2Ag_2Se_2$ consists of infinite sheets of CoO_2 with the Co^{2+} ions in an octahedral coordination environment surrounded by the four oxide anions and two Se anions [9]. However, in common with many members of this family, the CoO_4Se_2 octahedra are elongated so that the local coordination of the Co^{2+} ions tends towards a square planar configuration due to the proximity of four oxide ions. This elongated environment is known to have a significant impact on the effective magnetic moment of the Co ions, increasing it from the $3\mu_B$ predicted by spin only contributions due to the presence of unquenched angular momentum. The space group is $I4/mmm$ and the arrangement of ions in the unit cell is illustrated in Fig. 1(a).

Magnetic susceptibility data measured on $Sr_2CoO_2Ag_2Se_2$ exhibits an extremely broad maximum centred at 230 K, but extending from 150 K to above room temperature [10], characteristic of two-dimensional antiferromagnetic ordering resulting from strong intra-plane superexchange [11–13]. The first derivative of the magnetic susceptibility data revealed a maximum of 190 K which was assigned as the Néel temperature. Upon further cooling three-dimensional magnetism results from weaker inter-plane superexchange interactions. The magnetic structure of $Sr_2CoO_2Ag_2Se_2$ [Fig. 1(c)] was investigated with powder neutron diffraction and was found to be consistent with long range antiferromagnetic ordering of the Co^{2+} moments interacting via superexchange by intermediate oxide ions [10].

The magnetic structure is shown in Fig. 1(c), using the magnetic unit cell described in Fig. 1(b). The present work aims to further investigate the antiferromagnetic ordering in this compound using muon-spin rotation (μ^+SR), a local probe technique that has proved effective at studying magnetic properties in a very wide range of layered magnetic materials. Our experiments yield a value of T_N which is 30 K lower than that previously deduced from magnetic susceptibility measurements. By using density functional theory (DFT) calculations to identify the muon stopping locations and then employing dipole-field simulations to calculate the field experienced by the muon at that location, our results also provide a constraint for the magnetic structure of $Sr_2CoO_2Ag_2Se_2$.

II. EXPERIMENTAL DETAILS

Our sample of $Sr_2CoO_2Ag_2Se_2$ was made according to the procedure detailed in Ref. [10] which involved solid state sintering of a pressed pellet of Se, Co, Ag, and SrO. Pure SrO was prepared from thermal decomposition of $SrCO_3$ by he ating it for 18 h at 850°C and for a further 6 h at 1100°C under dynamic vacuum. The reactants were ground thoroughly in an argon-filled glove box and pressed into one pellet, then loaded into an alumina crucible. Finally, the crucible was sealed in a dried silica tube under vacuum and heated in a furnace for two days at 835°C. The sample was characterized by x-ray diffraction and powder neutron diffraction [10].

In a μ^+SR experiment [14], one implants spin-polarized positive muons into a sample of interest where they

*george.gill@physics.ox.ac.uk
†stephen.blundell@physics.ox.ac.uk

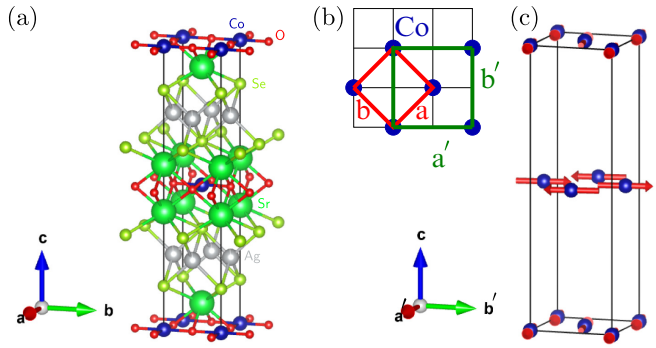

FIG. 1. (a) The crystal structure, (b) magnetic unit cell, and (c) magnetic structure of $Sr_2CoO_2Ag_2Se_2$. In (b) and (c), only the magnetic Co ions are shown for clarity. As illustrated in (b), the magnetic unit cell has axes denoted by a' and b' which are $\sqrt{2}$ times larger and rotated by 45 degrees with respect to a and b, the axes of the crystallographic unit cell. The magnetic structure is obtained from powder neutron diffraction studies reported in [4].

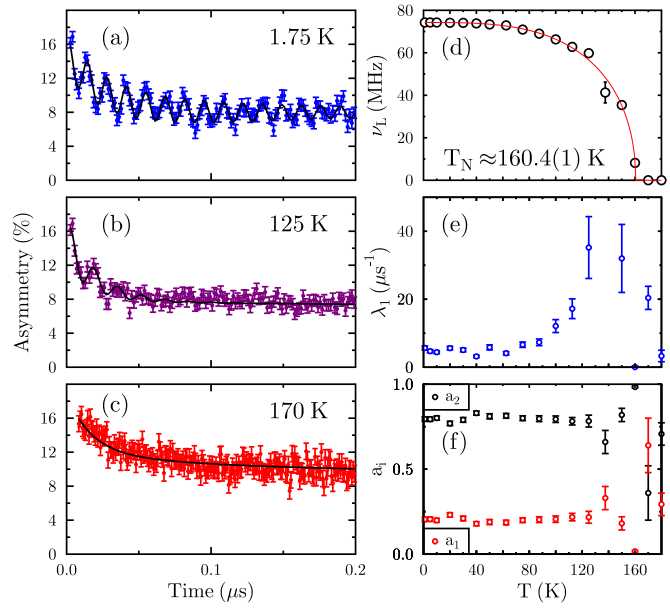

FIG. 2. ZF μ^+SR asymmetry data for $Sr_2CoO_2Ag_2Se_2$ measured for $T =$ (a) 1.75 K, (b) 125 K, and (c) 170 K. The fitted temperature dependence of the (d) precession frequency ν, (e) relaxation rate λ_1 and (f) amplitudes a_1 and a_2.

subsequently decay into a positron after a time t with a probability that is proportional to $e^{-t/\tau}$, where τ is the average lifetime of the muon. The decay positron is emitted preferentially in the direction of the muon's instantaneous spin direction, and the measured quantity of positron asymmetry $A(t)$ is proportional to the muon ensemble's spin polarization, the time dependence of which is sensitive to the local magnetic field experienced at the muon stopping site. We carried out zero-field (ZF) μ^+SR measurements on a polycrystalline sample of $Sr_2CoO_2Ag_2Se_2$ in a Quantum Continuous Flow Cryostat on the GPS spectrometer at the Swiss Muon Source, PSI Switzerland. The spin rotator was set to 45 degrees relative to the muon momentum. All muon data were analyzed with WiMDA [15].

III. RESULTS

The ZF asymmetry spectra for $Sr_2CoO_2Ag_2Se_2$ can be seen in Figs. 2(a)–2(c). One observes a clear oscillatory signal at 1.75 K and 125 K, which is indicative of long-range magnetic order, although the damping rate has increased at 125 K. We note that the asymmetry is ≈18% which is slightly lower than expected for the GPS instrument. We speculate that this missing fraction could be due to muonium formation. The data contains a single frequency, a significant relaxation that is characteristically Lorentzian, and a nonrelaxing component. The asymmetry signal $A(t)$ can be fitted to an expression given by $A(t) = A_r P(t) + A_0$, a sum of an oscillating and relaxing term $A_r P(t)$, and a nonrelaxing term A_0. Here A_0 and A_r are both temperature-independent constants and $P(t)$ is a function given by

$$P(t) = a_1 \cos(\omega_L t) e^{-\lambda_1 t} + a_2 e^{-\lambda_2 t}, \qquad (1)$$

where $\omega_L = \gamma_\mu B$ is the Larmor frequency, $\gamma_\mu = 2\pi \times 135.5$ MHz T^{-1} is the gyromagnetic ratio of the muon, and B is the magnetic field experienced by the muon at the stopping site. The experiment was carried out in flypast mode and so we can assume that the asymmetry signal results predominantly from muons stopped inside the sample. The oscillating part of that signal, represented by the fraction a_1 in Eq. (1), corresponds to muons experiencing a static magnetic field resulting from long range magnetic order inside the sample. The fraction represented by a_2 does not give rise to any oscillations, and therefore corresponds to muons experiencing only dynamical fluctuations of the moments, leading to a significant relaxation of their polarization as parametrized by the relaxation rate λ_2. There is also a sizable fraction of the muons which do not relax, corresponding to the constant term $A_0 \approx 10\%$. Some contributions to this term could arise from muons stopping in the sample holder, but we believe such an explanation could only apply to a very small fraction of A_0 and the remainder must be instrinsic to the sample. The fitted values of the temperature dependences of the frequency ν, relaxation rate λ_1, and amplitudes a_1 and a_2 are shown in Figs. 2(d)–2(f). (The value of the fast relaxing component λ_2 appeared to be roughly constant with temperature and so was fixed at a value of 66.1 MHz in all the fits, so this is not plotted.)

The temperature dependence of the Larmor frequency $\nu_L = \omega_L/(2\pi)$ is plotted in Fig. 2(d) and remains approximately constant at roughly 75 MHz until around 60 K where it starts to drop smoothly, eventually falling to zero above $T_N \approx 160$ K. In Fig. 2(d) the temperature dependence of the frequency is fitted to the phenomenological expression

$$\nu_L(T) = \nu_L(0)\left[1 - \left(\frac{T}{T_N}\right)^{\alpha}\right]^{\beta}, \qquad (2)$$

and allows the extraction of the Néel temperature $T_N = 160.4(1)$ K, which is around 30 K lower than that previously estimated from susceptibility measurements [10]. We note that those susceptibility measurements only identified a very broad maximum and revealed no sharp features in this low-dimensional compound that would indicate unambiguously a magnetic transition to a long-range ordered state. In con-

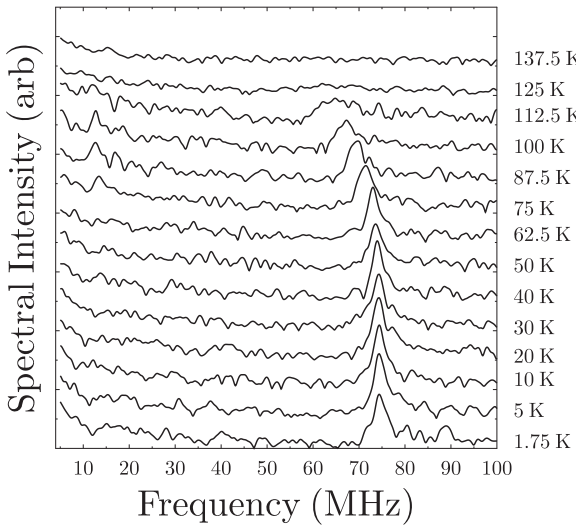

FIG. 3. Fourier spectra of the asymmetry data for $Sr_2CoO_2Ag_2Se_2$ at different temperatures.

trast, our μSR data reveal a clearly oscillating fraction with a well-defined frequency, and this frequency follows the order parameter and collapses on warming through the transition, providing a much more reliable estimate of T_N. The μSR experiment reveals this transition unmistakably and transparently, in a way that the susceptibility measurement with its broad transition cannot. Our fit yields a precession frequency extrapolated to zero temperature $\nu_L(0) = 74.24(4)$ MHz, as well as values for the critical exponents $\alpha = 3.23(9)$ and $\beta = 0.46(3)$. The extracted value for β is slightly larger than what one would expect from a 3D Heisenberg antiferromagnet, but this is only a crude estimate of the critical exponent due to the small number of data points around the transition temperature, and the fit given in Eq. (2) is phenomenological. However, the extracted value of $\nu_L(0)$ results from the dipolar field from the ordered spins acting at the muon site and will be extremely useful in our subsequent analysis.

Figure 3 shows the asymmetry spectra at different temperatures plotted in the frequency domain. There is a clear peak in the spectral intensity around 75 MHz which appears at lower temperature. As the temperature is increased, the frequency eventually broadens out and then largely disappears.

Figure 2(e) shows the temperature dependence of the relaxation rate λ_1. At low temperature λ_1 is roughly temperature independent and relaxing much slower than λ_2. As the temperature starts to increase above around 80 K, the relaxation rate starts increasing and reaches a broad peak around the Néel temperature. This correlates with the broadening of the peak in the Fourier spectrum (Fig. 3) and also with the disappearing of the oscillations in the asymmetry data [Figs. 2(b) and 2(c)]. Figure 2(f) shows the amplitudes of the oscillating component (a_1) and the fast relaxing component (a_2). We note that a_1 is much smaller than a_2, so that the fraction of muons sensitive to magnetic order is relatively small. The two amplitudes remain stable in the fits until the high temperature region is reached, at which point we deduce that Eq. (1) is no longer a good description of the data.

TABLE I. The first column in the table shows the muon positions in fractional coordinates for the lowest energy sites determined with DFT+μ. The second column gives the difference in energy between the sites, with the first entry being zero, i.e., the lowest energy configuration found. Finally, the third column shows the frequency that the muon precesses at due to the dipolar field experienced at the muon position.

Muon Position	Δ E (meV)	Frequency (MHz)
(0.507, 0.843, 0.544)	0	78
(0.656, 0.003, 0.956)	0.23	77
(0.484, 0.850, 0.454)	0.41	74

IV. DENSITY FUNCTIONAL THEORY AND DIPOLE FIELD CALCULATIONS

A difficulty one often faces in positive muon spin rotation experiments is that the muon stopping site is generally unknown. Another issue is the unknown extent to which the muon perturbs the local environment, especially in the region where the material of interest is suspected to order. In recent years, it was realised that density functional theory (DFT) could be a very powerful tool for characterizing these muon implantation sites and their effect on the crystal and electronic structure of the host material [16].

DFT calculations were carried out with the QUANTUM ESPRESSO [17] program using the generalized gradient approximation employed by Perdew, Burke, and Ernzernhofer [18]. The ions were modeled using ultrasoft pseudopotentials and the muon was modeled with an ultrasoft hydrogen pseudopotential. Firstly, a convergence test was conducted to find suitable values for the wave function and charge density cutoffs of 70 and 700 Ry, respectively (where Ry is the Rydberg constant). The k points were also subject to a convergence test for which a 6×6×2 Monkhorst-Pack k-space grid was found to yield the best results. These values were all used in subsequent calculations. To find the candidate muon positions, calculations on $Sr_2CoO_2Ag_2Se_2$ were conducted in a single conventional unit cell, where the total energy must converge to at least 10^{-6} Ry/atom. A diamagnetic muon (i.e., the total unit cell has charge +1) is then introduced into the cell and the system is allowed to relax fully until the forces acting on the atoms converge to below 10^{-3} Ry/a.u.

The optimal location of the muon was found to be (0.507, 0.843, 0.544) in fractional coordinates, located ≈1 Å away from the center of the nearest oxygen anion, which is typical for oxygen-containing systems. The lowest energy muon positions are summarized in Table I with their corresponding frequency. The second and third lowest energy sites actually correspond to frequencies closer to the experimentally measured value. The muons are sitting ≈1 Å away from the nearest oxygen ion for all of these configurations and the sites are all similar. Other sites were determined, but these higher-energy sites were ruled out as they were located close to positively charged cobalt ions, and dipole-field simulations predicted very large fields at those sites which are not observed in our data.The implantation of the muon breaks the local symmetry and perturbs the ions around it,

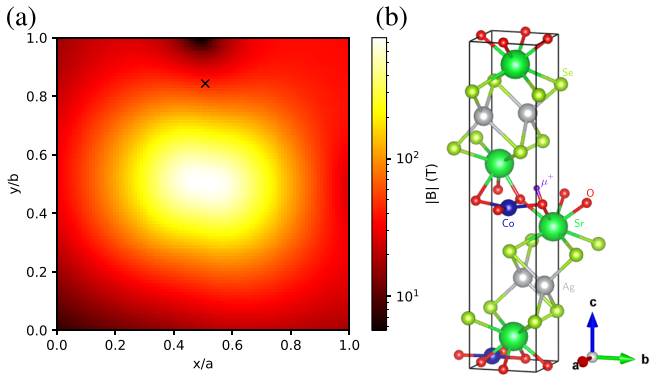

FIG. 4. (a) Heat map showing the magnitude of the magnetic field $|\mathbf{B}_\mu|$ across the *ab* plane (cross section taken at $c = 0.544$) from dipole field calculations using the spin configuration within the unit cell, and magnetic moment magnitude from [10]. The muon site determined by DFT calculations is shown as a black cross. (b) The structure of the distorted unit cell. The muon induces a structural perturbation removing the symmetry.

slightly changing the bond lengths and angles, and results in the configuration shown in Fig. 4(b).

To test the applicability of the magnetic structure proposed in [10] against the experimentally observed magnetic field strengths that the muons experience, magnetic dipole field calculations were performed at the muon stopping site. The dipolar field at position $\mathbf{r}$ is given by

$$B^\alpha(\mathbf{r}) = \frac{\mu_0}{4\pi} \sum_{i,\beta} \frac{\mu_i^\beta}{R_i^3} \left(\frac{3R_i^\alpha R_i^\beta}{R_i^2} - \delta^{\alpha\beta} \right), \tag{3}$$

where α and β run over the x, y, and z directions, i labels a magnetic ion which is located at position $\mathbf{r}_i$ and is within the Lorentz sphere centered at $\mathbf{r}$, $\mathbf{R}_i = \mathbf{r} - \mathbf{r}_i$, μ_i^β is the β component of the effective magnetic moment of ion i, and $\delta^{\alpha\beta}$ is the Kronecker delta (equal to one if $\alpha = \beta$ and zero otherwise). The sum in Eq. (3) is taken over the infinite lattice, but converges relatively quickly if one takes a Lorentz sphere of sufficiently large radius [19]. Because of the antiferromagnetic spin structure there is no contribution from the Lorentz field or from demagnetization fields. Assuming the spin structure shown in Fig. 1(c) and the magnetic moment magnitude of $3.7\mu_B$ [10], evaluation of Eq. (3) yields an estimate of the magnetic field at the muon site $B_\mu = 0.576$ T, corresponding to a precession frequency of 78 MHz. The field experimentally observed at low temperature is very slightly lower than this value at 0.55 T, corresponding to a frequency of 75 MHz, but the two values are in pretty good agreement. Figure 4(a) shows the magnitude of the magnetic field strength $|\mathbf{B}_\mu|$ within the *ab* plane for $c = 0.544$ (the z position of the muon). The black cross marks the position of the muon in the plane. The local field varies markedly around this region, so that a small change in muon site would lead to a large change in local field. Since muon sites are not determined to better than about 0.1 Å at best, the agreement between predicted field and measured field demonstrates that the candidate muon site is indeed plausible.

It is worth noting that the authors chose the magnetic structure [10] with a 90° rotation of the spins between layers because it allowed the retention of the tetragonal symmetry. A further test to check whether this structure is consistent is to compute the dipole field at the muon site with a 0° rotation of the spins between layers. Doing so gives a value of 0.32 T, corresponding to a frequency of 43 MHz. This difference adds further evidence for the magnetic structure proposed in [10]. Furthermore, this rotation of 90° between layers could be responsible for the broadening of the frequency in Fig. 3. Above 120 K where the precession signal broadens considerably, it could be that large interlayer fluctuations could cause a loss of coherence between the 90°orientation of the planes, leading to rapidly changing local fields which could explain our observations. Detailed examination of the Bragg peaks measured in neutron diffraction in this temperature range could provide further evidence of this proposed effect.

However, it might also be that such fluctuations could be responsible for giving rise to the nonoscillating part of the muon data (either the exponentially relaxing or nonrelaxing components) for which we do not find a persuasive alternative explanation. The low-energy sites identified by DFT calculations are all consistent with a magnetically ordered fraction with a frequency in agreement with our experimental results. This would then lead to a $\frac{2}{3}$ oscillating part and a $\frac{1}{3}$ relaxing part, so that we would expect the oscillating fraction to have twice the amplitude of the relaxing part. Our data reveals a much larger nonoscillating part, the origin of which we cannot otherwise explain. The neutron diffraction data shows that the sample is single phase and the magnetic order welldefined, but the refined magnetic structure is a mixture of the $mX3^+(a)$ and $mX4^+(a)$ modes, meaning that tetragonal symmetry is retained by mixing the configuration shown in Fig. 1(c) with one rotated by 90° about the c axis [10]. We speculate that the nonoscillatory components might be associated with this degree of freedom in the local magnetic structure.

V. CONCLUSION

Bulk magnetic susceptibility experiments on $Sr_2CoO_2Ag_2Se_2$ and related materials often do not show a clear signature of three-dimensional long range antiferromagnetic ordering. Our μSR data reveals a clear oscillatory signal which on warming collapses unambiguously at the ordering transition and provides a more reliable estimate of T_N in this compound than has been possible with measurements of bulk magnetic susceptibility which appear to substantially overestimate the ordering temperature. Furthermore, the likely stopping site of the muon in $Sr_2CoO_2Ag_2Se_2$ has been identified and allows us to predict a local magnetic field at the muon site, corresponding to a muon precession frequency of 78 MHz at low temperature. This result is consistent with the magnetic structure proposed in Ref. [10]. Our results also provide evidence for a loss of coherence between the 90° orientation of layers that may be responsible for the large nonrelaxing component in the muon data and may contribute to the broadening of the precession signal and rapidly increasing relax ation rate that is observed just below T_N.

ACKNOWLEDGMENTS

Muon measurements were made at the Swiss Muon Source and we thank PSI for the provision of beamtime, and Chennan Wang for excellent technical support. We are grateful to EPSRC (UK) for financial support (EP/N023803/1, EP/T027991/1 and EP/P018874/1).

[1] W. J. Zhu, P. H. Hor, A. J. Jacobson, G. Crisci, T. A. Albright, S. H. Wang, and T. Vogt, J. Am. Chem. Soc. **119**, 12398 (1997).
[2] S. J. Clarke, P. Adamson, S. J. C. Herkelrath, O. J. Rutt, D. R. Parker, M. J. Pitcher, and C. F. Smura, Inorg. Chem. **47**, 8473 (2008).
[3] J. N. Blandy, A. M. Abakumov, K. E. Christensen, J. Hadermann, P. Adamson, S. J. Cassidy, S. Ramos, D. G. Free, H. Cohen, D. N. Woodruff, A. L. Thompson, and S. J. Clarke, APL Mater. **3**, 041520 (2015).
[4] Z. A. Gál, O. J. Rutt, C. F. Smura, T. P. Overton, N. Barrier, S. J. Clarke, and J. Hadermann, J. Am. Chem. Soc. **128**, 8530 (2006).
[5] J. N. Blandy, J. C. Boskovic, and S. J. Clarke, J. Solid State Chem. **245**, 61 (2017).
[6] J. N. Blandy, S. Liu, C. F. Smura, S. J. Cassidy, D. N. Woodruff, J. E. McGrady, and S. J. Clarke, Inorg. Chem. **57**, 15379 (2018).
[7] C. F. Smura, D. R. Parker, M. Zbiri, M. R. Johnson, Z. A. Gal, and S. J. Clarke, J. Am. Chem. Soc. **133**, 2691 (2011).
[8] E. Brechtel, G. Cordier, and H. Schäfer, Z. Naturforsch. B **34**, 777 (1979).
[9] S. Jin, X. Chen, J. Guo, M. Lei, J. Lin, J. Xu, W. Wang, and W. Wang, Inorg. Chem. **51**, 10185 (2012).
[10] S. J. C. Herkelrath, J. N. Blandy, and S. J. Clarke, J. Solid State Chem. **264**, 119 (2018).
[11] C. S. Knee, D. J. Price, M. R. Lees, and M. T. Weller, Phys. Rev. B **68**, 174407 (2003).
[12] J. B. He, D. M. Wang, H. L. Shi, H. X. Yang, J. Q. Li, and G. F. Chen, Phys. Rev. B **84**, 205212 (2011).
[13] N. Ni, E. Climent-Pascual, S. Jia, Q. Huang, and R. J. Cava, Phys. Rev. B **82**, 214419 (2010).
[14] S. J. Blundell, Contemp. Phys. **40**, 175 (1999).
[15] F. L. Pratt, Phys. B: Condens. Matter **289-290**, 710 (2000).
[16] J. S. Möller, P. Bonfà, D. Ceresoli, F. Bernardini, S. J. Blundell, T. Lancaster, R. De Renzi, N. Marzari, I. Watanabe, and S. Sulaiman, Phys. Scr. **88**, 068510 (2013).
[17] P. Giannozzi, S. Baroni, N. Bonini, M. Calandra, R. Car, C. Cavazzoni, D. Ceresoli, G. Chiarotti, M. Cococcioni, I. Dabo, A. D. Corso, S. de Gironcoli, S. Fabris, G. Fratesi, R. Gebauer, U. Gerstmann, C. Gougoussis, A. Kokalj, M. Lazzeri, L. Martin-Samos, N. Marzari *et al.*, J. Phys.: Condens. Matter **21**, 395502 (2009).
[18] J. P. Perdew, K. Burke, and M. Ernzerhof, Phys. Rev. Lett. **77**, 3865 (1996).
[19] L. W. McKeehan, Phys. Rev. **43**, 913 (1933).